



Changes in the structural and electrophysical properties of $\text{Ba}_{0.8}\text{Sr}_{0.2}\text{TiO}_3$ films with decreasing thickness

Evgeny I. Goldman, Galina V. Chucheva, Mikhail S. Afanasiev, Dmitry A. Kiselev*

Laboratory «research of physical phenomena on the surface and interfaces of solids», Fryazino Branch of the Kotelnikov Institute of Radioengineering and Electronics of Russian Academy of Sciences, Vvedensky sq. 1, Fryazino, Moscow region, 141190, Russia

ARTICLE INFO

Article history:

Received 24 July 2020

Revised 18 September 2020

Accepted 23 September 2020

Keywords:

BSTO ferroelectric thin films

The morphology

Domain switching

Dielectric properties

The thickness effect

High-frequency capacitance–voltage characteristics

ABSTRACT

Comparative studies of structural and electrophysical properties were performed for $\text{Ba}_{0.8}\text{Sr}_{0.2}\text{TiO}_3$ (BSTO) films with the thickness of 100 nm, 120 nm and 350 nm. The surface morphology, the domain structure and local polarization switches were explored in the ferroelectric phase whereas high-frequency capacitance–voltage characteristics were measured in the paraelectric phase at 121°C. It was shown that good crystalline properties of the BSTO surface and grains are preserved until the thickness of ceramic layers decrease to 100 nm. The surface roughness did not exceed 2 – 4 nm and the average radius grains was in the range of 64 – 87 nm. Polarization domains induced with a microscope tip were stable and are conserved for several hours. Electrophysical properties of $\text{Ba}_{0.8}\text{Sr}_{0.2}\text{TiO}_3$ films in the paraelectric phase strongly depend on the thickness of layers of BSTO ceramics. Effective dielectric permittivity of BSTO in the limit of weak fields decreases when the film thickness decreases from 350 nm to 100 nm from 920 to 400.

© 2020 Elsevier Ltd. All rights reserved.

1. Introduction

The main element widely used in different areas of studies in adjustable logical devices and neuromorphic networks are memristors, i.e., structures capable to multiple switches between states with high and low resistance after applications of the external voltage of the different polarity. In the last decade, it became clear [1] that the perspective direction of increasing material resources for fabricating memristors are thin films of solid solutions of barium-strontium titanates ($\text{Ba}_{1-x}\text{Sr}_x\text{TiO}_3$ or BSTO). These films possess ferroelectric properties at the room temperature and their dielectric permittivity remains to be high in a wide temperature range. BSTO-based structures are already used in energy-independent memory devices which are resistant to special impacts [2]; however, not much is known about properties of BSTO films, in particular, in the thickness range of 100 nm. This range is especially important since films with such thickness, including BSTO films, begin to show a memristor behavior [3]. It was previously shown that properties of films and bulky $\text{Ba}_{1-x}\text{Sr}_x\text{TiO}_3$ particles are different [4,5]; therefore, it is important to determine how structural and electrophysical characteristics of BSTO layers depend on thickness decrease up to 100 nm. Electrophysical properties of ferroelectric structures, which are dependencies of high-frequency

capacitance on external voltage, are described by coefficients of the free energy F expansion in powers of the order parameter – the electric polarization of a material P . Distributions over domains of the spontaneous polarization of materials occur in the ferroelectric phase [6]; therefore, the dependence of capacitance of a ferroelectric film on the applied voltage should include three-dimensional averaging of the domain polarization over space. There is no spontaneous polarization in a paraelectric phase and the account of polarization distributions over space is substantially simplified and the problem becomes one-dimensional as it was underlined previously [7].

The present work is devoted to a comparative study of structural and electrophysical properties of $\text{Ba}_{0.8}\text{Sr}_{0.2}\text{TiO}_3$ films with the thickness of 100 nm, 120 nm and 350 nm. The surface morphology, the domain structure and switches of the local polarization of films have been explored at room temperature whereas high-frequency capacitance–voltage characteristics (C-V) were measured in the paraelectric region at 121°C.

2. Experimental technique

Metal-BSTO-metal samples with ceramic layers of various thickness were prepared on a silicon substrate with a platinum sublayer whose thickness was ~200 nm. Ferroelectric $\text{Ba}_{0.8}\text{Sr}_{0.2}\text{TiO}_3$ films were deposited onto a platinum electrode using high-frequency spray of polycrystalline target in an oxygen atmosphere using an

* Corresponding author.

E-mail address: dm.kiselev@gmail.com (D.A. Kiselev).

installation Plasma-50SE (Russia). The temperature of the substrate during the synthesis process was maintained at $620 \pm 5^\circ\text{C}$. The process consisted of two stages. At the first one, the material was precipitated for six or more minutes in the dependence on the required layer thickness. At the second stage, films obtained were treated thermally in an oxygen atmosphere and the chamber pressure of 10^4 Pa. The upper electrode (which was missing during the structural exploration) on a ferroelectric film was prepared by electron-beam spray of nickel via a shadow mask on an installation A700QE/DI12000 (Germany). The electrode area S and its thickness were 2.7×10^{-4} cm² and 0.1 μm , respectively. The design of installations and the technique of the film deposition are described in more detail elsewhere [8,9]. The relationship between thicknesses of BSTO films and the deposition time of the material was determined using a scanning electron microscope SU5000.

The surface morphology, the induced domain structure and local polarization switching of thin films were investigated using Piezoresponse Force Microscopy (PFM) and scanning probe microscope MFP-3D (Asylum Research, Oxford Instruments, Santa Barbara, CA, USA) with a Ti/Ir coated Si cantilever (Asylec-01, Asylum Research, Oxford Instruments, USA) and a nominal 2.5 N/m spring constant. Switching spectroscopy PFM (SS-PFM) measurements were performed with a 9 V bias to the tip. An AC voltage (2 V_{pp}) was superimposed onto a triangular square-stepping wave ($f = 0.5$ Hz, with writing and reading times 25 ms, and bias window up to ± 9 V) during the remnant piezoelectric hysteresis loops measurements.

Capacitance–voltage (C-V) characteristics measurements of Ni-BSTO-Pt structures were performed on an automated stand [10] us-

ing an LCR Agilent E4980A precision meter. A bias voltage V_g ranged from -3.5 to $+3.5$ V was applied to the sample with a step of 5 mV and the amplitude and frequency of the measuring signal of 25 mV and 100 kHz, respectively.

3. Results and discussion

3.1. Structural topography

The surface morphology of BSTO films deposited on the Pt/TiO₂/SiO₂/Si substrates with different thickness is shown in Fig. 1a and 1b. As can be seen, BSTO films possess by comparatively homogeneous and smooth surfaces and are formed from crystallites (grains). The average roughness increased from 2 nm for the 100 nm thick BSTO film to 4 nm in the 120 nm thick BSTO film. To quantify the grain size (correlation length, ξ), we used the autocorrelation function and the algorithm of calculations described elsewhere [11]. According to results of our calculations, the mean radius of grains increases from 64.4 nm in the 100 nm thick BSTO film to 87.2 nm in the 120 nm thick BSTO film (see Fig. 1c). Thus, it can be concluded that relatively dense microstructures are beneficial to their ferroelectric, dielectric and piezoelectric properties. Previously, we have experimentally established that the average grain size for a film with thickness of 350 nm is also 87 nm [11]. Therefore, one can consider that grains in BSTO films, synthesized using our method described above, have a columnar arrangement, and they grow laterally only to a certain size when the film thickness increases.

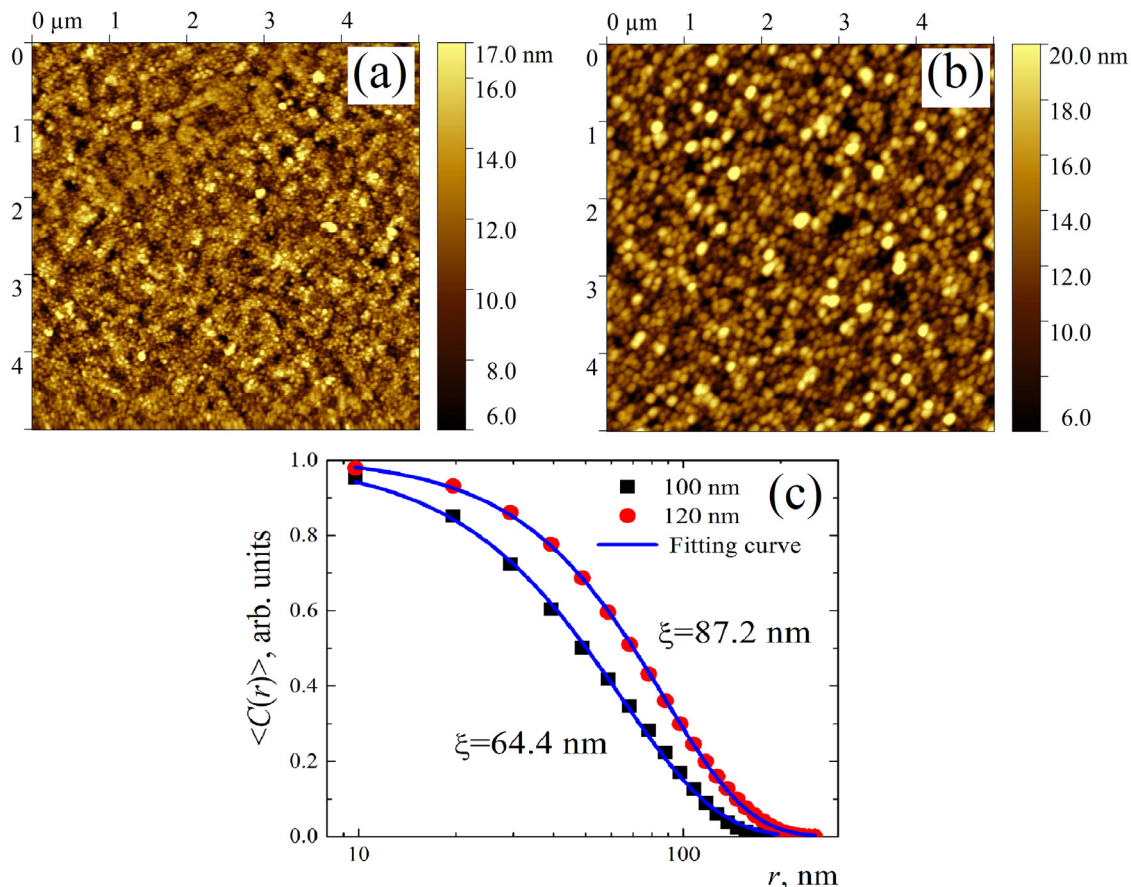


Fig. 1. Surface images of BSTO films with the various thickness (a) – 100 nm, (b) – 120 nm and (c) – profiles of the autocorrelation function (points) and their approximation (lines) for BSTO films under study. Lines show the fit of experimental points to the equation $C(r) = A \cdot \exp[-(r/\xi)^{2.1}]$.

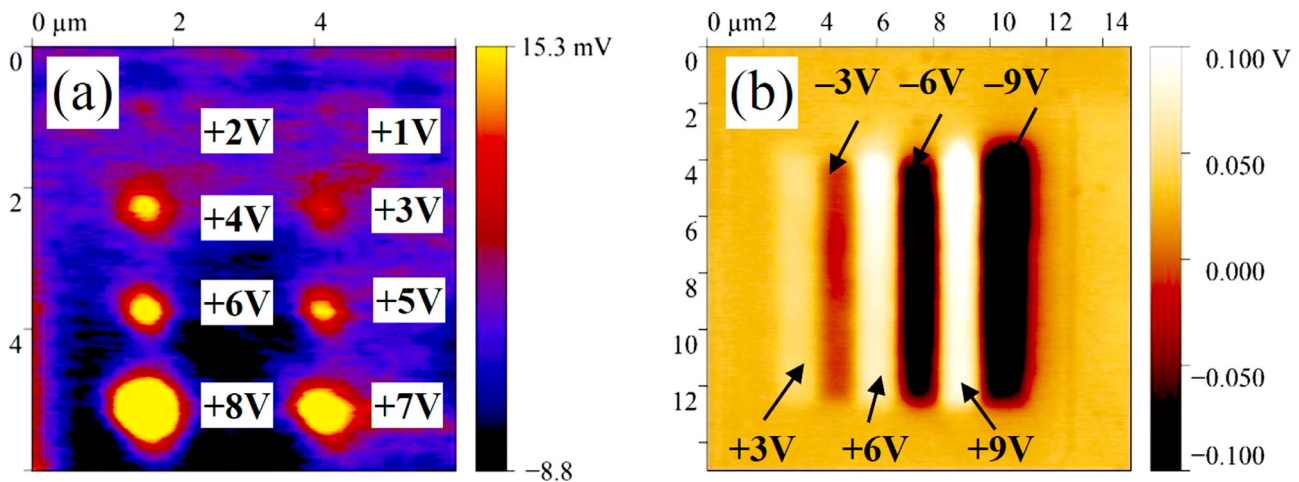


Fig. 2. PFM images of dot patterned domains formed by positive voltage pulses with the different amplitude for the BSTO film with the thickness 100 nm (a) and induced strip domain regions by different voltage for 120 nm thick BSTO layer (b).

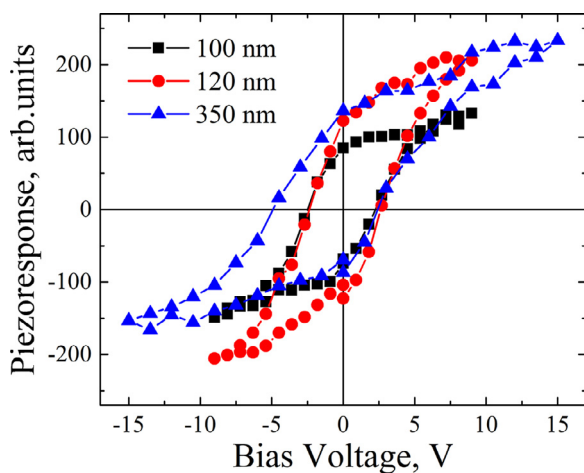


Fig. 3. Remnant PFM hysteresis loops for investigated BSTO film with different thickness.

3.2. Polarization switching at nanoscale

In order to further study the domain switching behavior of BSTO films, electrical poling was performed by scanning in write domain mode with a conductive probe, which applying up to ± 9 V DC bias on the tip. Fig. 2(a) shows the piezoresponse image of an array of eight domains created by applying voltage pulses ranging from +1 V to +8 V with fixed time 60 s. It can be seen that the domain diameter D strongly depends on magnitude of the voltage pulse applied between the PFM tip and the bottom electrode. Created domains demonstrate high stability for several hours.

Along with local (“point”) polarization, we experimentally investigated the polarization in a $9 \times 9 \mu\text{m}^2$ area of 120 nm thick BSTO film (Fig. 2(b)). The investigated area was divided into six strips with a width of $1 \mu\text{m}$ and a length of $9 \mu\text{m}$, which were polarized by a DC voltage V_g of ± 3 , ± 6 , and ± 9 V applied between the cantilever and the sample. Then, a $15 \times 15 \mu\text{m}^2$ area containing the polarized region was studied by PFM. Regions polarized by different voltages can be seen as pronounced strips. Light and dark strips correspond to different directions of the polarization vector. The contrast of signals from polarized regions, which corresponds to the piezoresponse signal amplitude, increases with polarizing potential.

In addition, Fig. 3 illustrates remnant (off-field) piezoresponse loops for three samples with the different thickness. The presence of hysteresis loops confirms the effect of polarization switching in BSTO thin films. The nominal amplitude data reflect the longitudinal piezoelectric response (d_{33}). Hysteresis loops explicitly shows the thickness (and grain size) dependence of the local piezoresponse for BSTO films.

It can be seen that coercive voltages for samples 100 and 120 nm thick are the same ($V_{C+} \sim 2$ V, $V_{C-} \sim -2.5$ V). But, for films under study, piezoelectric hysteresis loops have an asymmetric shape. Shifts reflect the induced interface electrostatic potential step due to the built-in electric field [12], due to both structural defects in the BSTO and surface states at the interface boundaries. The greatest asymmetry is observed for the thick sample BSTO 350 nm: $V_{C+} \sim 2.4$ V, $V_{C-} \sim -5$ V. However, one can clearly see a difference between the remnant piezoresponse signal measured at maximum voltage ($V_g = V_{max}$) and after removal of the polarizing voltage ($V_g = 0$ V); piezoresponse values for the BSTO film with thickness 120 nm and 350 nm, are larger than those for the 100 nm thick film. The increase of the grain size with increasing thickness coincides with the increase of piezoelectric properties, in agreement with the dielectric grain-size effect.

3.3. Study of capacitance–voltage characteristics

Fig. 4 presents C–V-characteristics $C(V_g)$ of studied structures. The voltage V_{gmax} in points of maxima in the figure has to be defined by the difference in work functions of metal contacts and BSTO films. The difference between V_{gmax} values of three curves in Fig. 4 is about 0.2 V which indicates that there are contributions from lagging effects in the process of dynamic measurements.

In the framework of the Landau theory of phase transitions of the second order without accounting for correlation effects, there were obtained [13] phenomenological expressions relating capacitance of a film in the paraelectric phase with coefficients of the expansion of the free energy density over power series expansion with respect to the polarization of a material:

$$F = F_0 + \frac{2\pi}{k} P^2 + \frac{A}{4} \frac{P^4}{P_0^2} - EP, \tag{1}$$

where F_0 is the free energy density in the absence of the polarization (i.e., without electrical forces); $4\pi/k$ is the inverse susceptibility, E is the electric field averaged on scale of a crystalline cell; $P_0 = q/a^2$, q is the elementary charge, a is the characteristic cell size, A is a dimensionless coefficient of the order of unity. It was

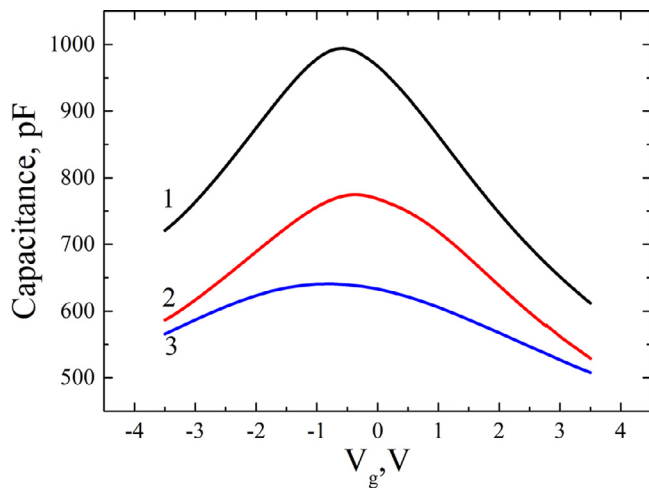


Fig. 4. High-frequency capacitance-voltage characteristics of Ni-BSTO-Pt structures. Curves of 1, 2, 3 correspond to thicknesses of BSTO layers 100, 120, 350 nm respectively.

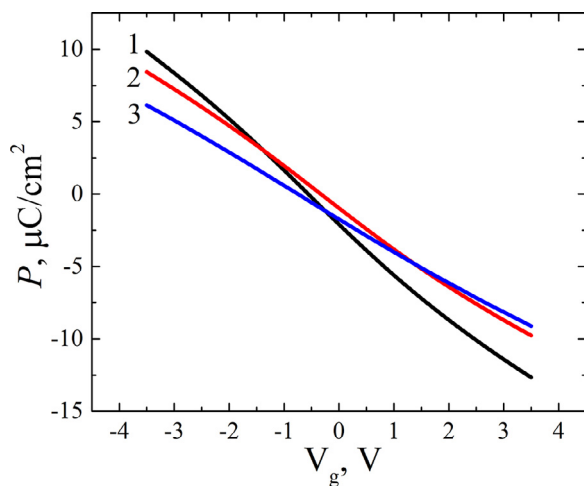


Fig. 5. The dependence of the polarization of BSTO films on the voltage of Ni-BSTO-Pt structures. Curves 1, 2, 3 correspond to the thicknesses of the BSTO layers 100, 120, 350 nm respectively.

shown [13] that if the condition $(AP^2/4\pi P_0^2) \ll 1$ is fulfilled in experiments then the maximal value of the capacitance can be expressed via the formula for a flat capacitor $C_{\max} = S(k+1)/4\pi h$, and the polarization can be computed according to the expression:

$$P(V_g) = \frac{k}{4\pi h} \times \left\{ 1 + \frac{(k+4)}{3(k+3)} \left[\frac{C_{\max}}{C(V_g)} - 1 \right] \right\}^{-1} (V_{g\max} - V_g). \quad (2)$$

k values defined using C_{\max} values (note that in the limit of small fields the $k+1$ parameter value equals the dielectric permittivity of BSTO) are $k = 400$ for 100 nm, $k = 425$ for 120 nm, and $k = 920$ for 350 nm. Therefore, ceramics quality strongly depends on a film thickness. The dependence of the polarization of a BSTO layer computed according to Eq. (2) as a function of external voltage is shown in Fig. 5. As can be seen, non-linearity of $P(V_g)$ functions appear at much larger displacements in the case of thick BSTO films than in thin ones. If to compare the polarization of samples in the same external fields i.e., at the same $(V_{g\max} - V_g)/h$ values, then P values of thick films are larger than those of thin films. This is a consequence of a substantial decrease in the coefficient k values when the thickness of a BSTO layer decreases.

4. Conclusion

Our studies of the morphology and ferroelectric properties of $\text{Ba}_{0.8}\text{Sr}_{0.2}\text{TiO}_3$ films have shown that good crystalline properties of the BSTO surface and grains are preserved until the thickness of ceramic layers decrease to 100 nm. The surface roughness did not exceed 2–4 nm and the average radius of grains was in the range of 64–87 nm. Crystallites had the shape of cylinders and they traverse the entire thickness of films. Polarization domains induced with a microscope tip were stable and are conserved for several hours. Electrophysical properties of the $\text{Ba}_{0.8}\text{Sr}_{0.2}\text{TiO}_3$ films in the paraelectric phase strongly depend on the thickness of layers in the BSTO ceramics. The effective dielectric permittivity of BSTO in the limit of weak fields decreases from 920 to 400 when the film thickness decreases from 350 nm to 100 nm. Under the same external electric fields, this leads to smaller polarization of thin films compared to thick ones.

Declaration of Competing Interest

Authors declare that they have no known competing financial interests or personal relationships that could have appeared to influence the work reported in this paper.

CRediT authorship contribution statement

Evgeny I. Goldman: Conceptualization, Writing - original draft, Writing - review & editing. **Galina V. Chucheva:** Conceptualization, Investigation, Supervision, Writing - review & editing. **Mikhail S. Afanasiev:** Methodology, Writing - review & editing. **Dmitry A. Kiselev:** Conceptualization, Investigation, Writing - original draft, Writing - review & editing.

Acknowledgments

This work was carried out as part of a state assignment and was partially supported by the Russian Foundation for Basic Research (projects 18-29-11029, 19-07-00271 and 19-29-03042). The authors are grateful to A.A. Sivov and D.A. Belorusov for help in C-V measurements of BSTO films.

References

- [1] Dawber M, Rabe KM, Scott JF. Rev. Mod. Phys 2005;77(4):1083. doi:10.1103/RevModPhys.77.1083.
- [2] Setter N, Damjanovic D, Eng L, Fox G, Gevorgian S, Hong S, Kingon A, Kohlstedt H, Park NY, Stephenson GB, Stoltichnov I, Taganstev AK, Taylor DV, Yamada T, Streiffer S. J. Appl. Phys 2006;100:051606. doi:10.1063/1.2336999.
- [3] Ma Zh, Li L, Wang Y, Zhou P, Guo Y, Liu Y, Liang K, Qi Y, Zhang T. Appl. Phys. Lett 2020;116:032903. doi:10.1063/1.5141903.
- [4] Biryukov SV, Mukhortov VM, Margolin AM, Golovko YuI, Zaharchenko IN, Dudkevich VP, et al. Ferroelectrics 1984;56(1–2):115. doi:10.1080/00150198408012733.
- [5] Shaw TM, Suo Z, Huang M, Liniger E, Laibowitz RB, Baniecki JD. Appl. Phys. Lett 1999;75:2129. doi:10.1063/1.124939.
- [6] Landau LD, Lifshits EM. Theoretical physics. viii electrostatics of continuous media. Moscow: Science; 2017.
- [7] Reich KV, Schechter M, Shklovskii BI. Phys. Rev. B 2015;91:115303. doi:10.1103/PhysRevB.91.115303.
- [8] Ivanov MS, Afanasiev MS. Phys. Solid State 2015;51(7):1259. doi:10.1134/S1063783409070026.
- [9] Kiselev DA, Afanasiev MS, Levashov SA, Chucheva GV. Phys. Solid State 2015;57(6):1151. doi:10.1134/S1063783415060189.
- [10] Goldman EI, Zhdan AG, Chucheva GV. Instrum. Exp. Tech 1997;40(6):841.
- [11] Afanasiev MS, Kiselev DA, Levashov SA, Sivov AA, Chucheva GV. Phys. Solid State 2019;61(10):1910. doi:10.1134/S1063783419100032.
- [12] Miao P, Zhao Y, Luo N, Zhao D, Chen A, Sun Z, et al. Sci Rep 2016;6:19965. doi:10.1038/srep19965.
- [13] Goldman EI, Naryshkina VG, Chucheva GV. Phys. Solid State 2020;62(8):1226. doi:10.1134/S1063783420080168.